



# Rainfall Microwave Spectral Atoms: A new Variational Approach for Combined Passive Retrievals



## Goal and Motivation

Developing state-of-the-art variational inversion techniques to enhance quality of precipitation passive/active retrievals in GPM era. The objectives are:

- 1) Improve quality of light and extreme precipitation retrievals over radiometrically complex land surfaces.
- 2) Develop a new combined variational formalism for simultaneous retrieval and fusion of multi-platform active-passive precipitation data.
- 3) Explore new approximation methodologies to obtain compact but effective representations of the  $\alpha$ -priori databases to provide insights for generation of compact but representative physically based  $\alpha$ -priori database, especially over land.

## ShARP: Shrunken LLE for Precipitation Retrieval

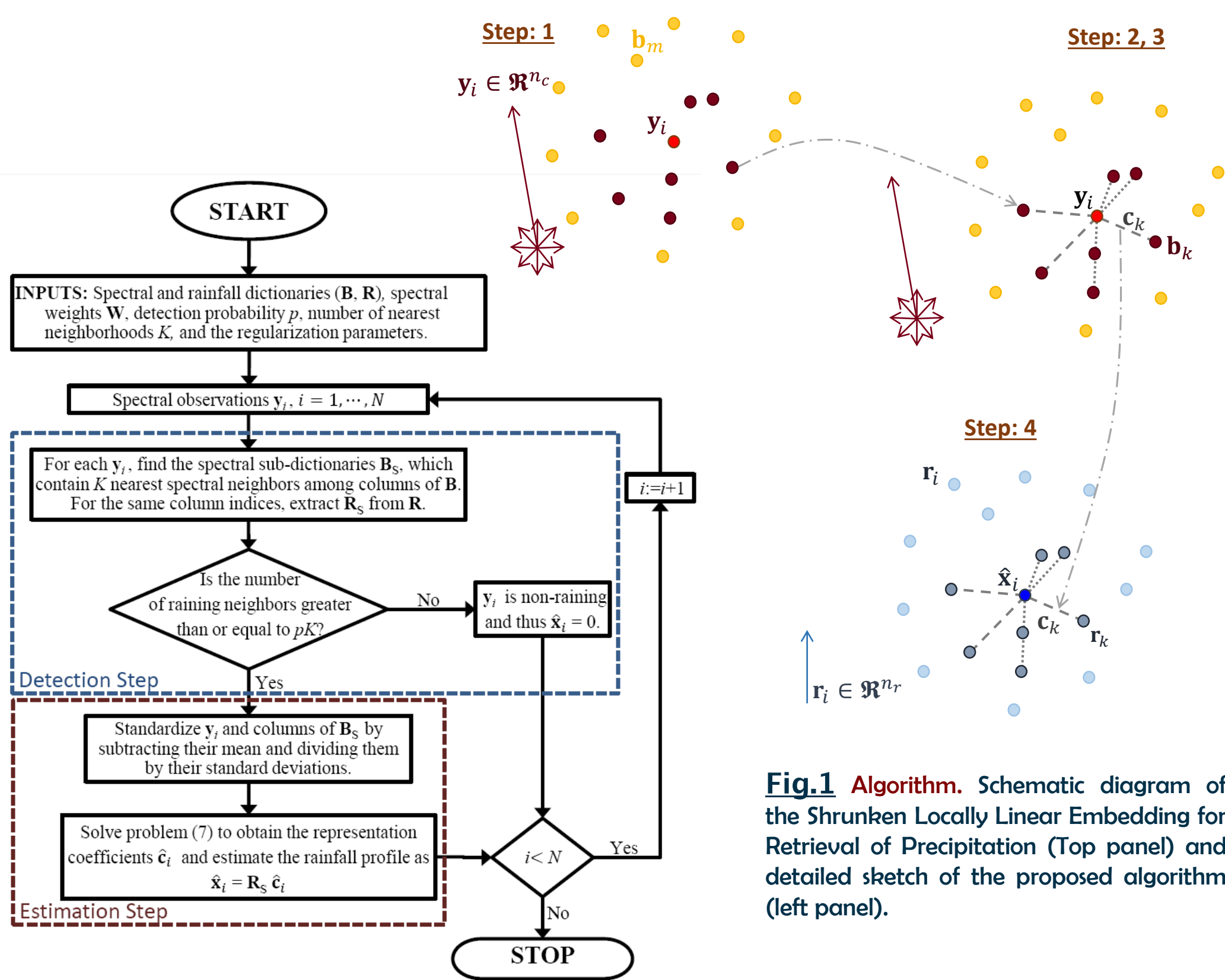


Fig.1 Algorithm. Schematic diagram of the Shrunken Locally Linear Embedding for Retrieval of Precipitation (Top panel) and detailed sketch of the proposed algorithm (left panel).

Algorithm 1 Shrunken Locally Linear Embedding Algorithm for Retrieval of Precipitation (ShARP).

Input: Spectral observations  $\{y_i = [y_{i1}, y_{i2}, \dots, y_{in}]^T \in \mathbb{R}^{n_s \times N}$ , vectors of spectral brightness temperatures, spectral  $B \in \mathbb{R}^{n_s \times M}$  and rainfall  $R \in \mathbb{R}^{n_r \times M}$  dictionaries, weight matrix  $W \in \mathbb{R}^{n_s \times n_r}$ , detection probability  $p$ , number of nearest neighbors  $K$ , and regularization parameters  $\lambda_1, \lambda_2$ .

Output: Precipitation field  $X$  containing  $\{x_i \in \mathbb{R}^{n_r}\}_{i=1}^N$  pixels of rainfall intensity profiles.

For  $i = 1$  to  $N$  step 1 do

- Find sub-dictionaries  $B_S \in \mathbb{R}^{n_s \times K}$  and  $R_S \in \mathbb{R}^{n_r \times K}$ , where  $S$  is the set of column indices of  $B$  which contains the  $K$ -nearest neighborhoods of  $y_i$ .
- Let  $R_S(\text{end}, :)$  denotes the last row of  $R_S$  containing neighboring surface rainfall.
- If  $\lfloor \text{supp}(R_S(\text{end}, :)) \rfloor \geq pK$ ,
  - Standardize  $y_i$  and atoms of  $B_S$ , such that  $\sum_{j=1}^K b_{ij} = 0$ ,  $\sum_{j=1}^K b_{jk} = 0$ , and  $\sum_{j=1}^K b_{jk}^2 = 1$ , for  $k = 1, \dots, K$ .
  - $c_i = \arg \min_{c_i \geq 0, 1^T c_i = 1} \left\{ \|W^{1/2}(y_i - B_S c_i)\|_2^2 + \lambda_1 \|c_i\|_1 + \lambda_2 \|c_i\|_2^2 \right\}$
  - $x_i = R_S c_i$
  - else
  - $x_i = 0$

End If

End For

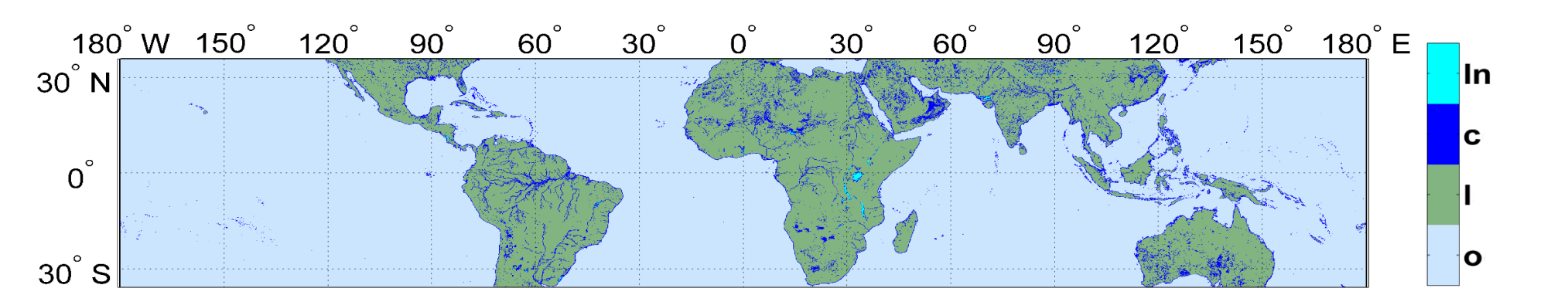


Fig.2 Different earth surface classes used in the current version of the ShARP, namely inland water body (ln), coastal zone (c), land (l) and ocean (o). The classification is adopted based on the available data (version 7) of the PR-IC21 product, mapped onto a 0.05-degree regular grid.

## Channel weights and signal-to-noise ratio

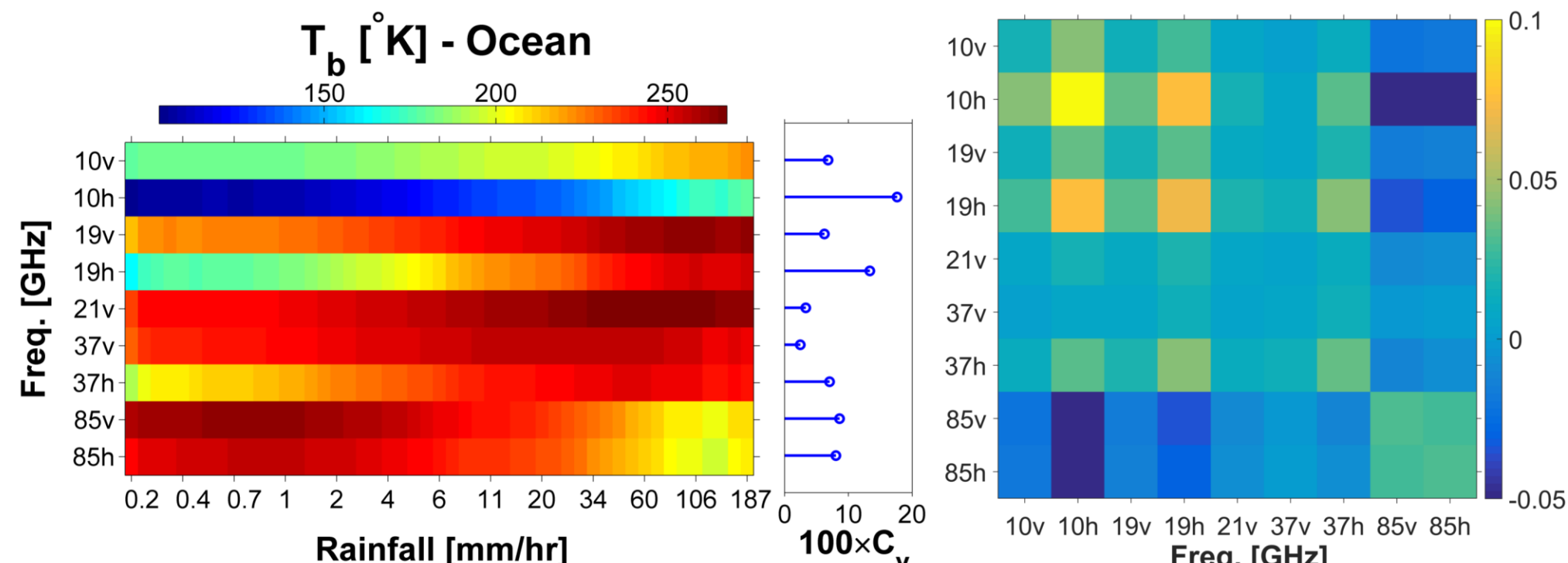


Fig.3 Incorporating cross-channel errors in retrieval. Expected values of spectral brightness temperatures for different intervals of the surface rainfall intensity over ocean (left panel). The stem plot demonstrates the coefficients of variation for each spectral band in response to the underlying rainfall variability. Note that the rainfall intervals on the x-axis are logarithmically spaced between 0.2 and 200 mm/h. Right panel: the image of the square root of the TMI channel precision matrix over ocean considering cross channel correlations. The weights are inferred from coincident pairs of the TMI-IB1 and PR-2A25 products obtained from 1000 randomly chosen orbits in five years.

## ShARP: Storm-scale and Global Retrievals

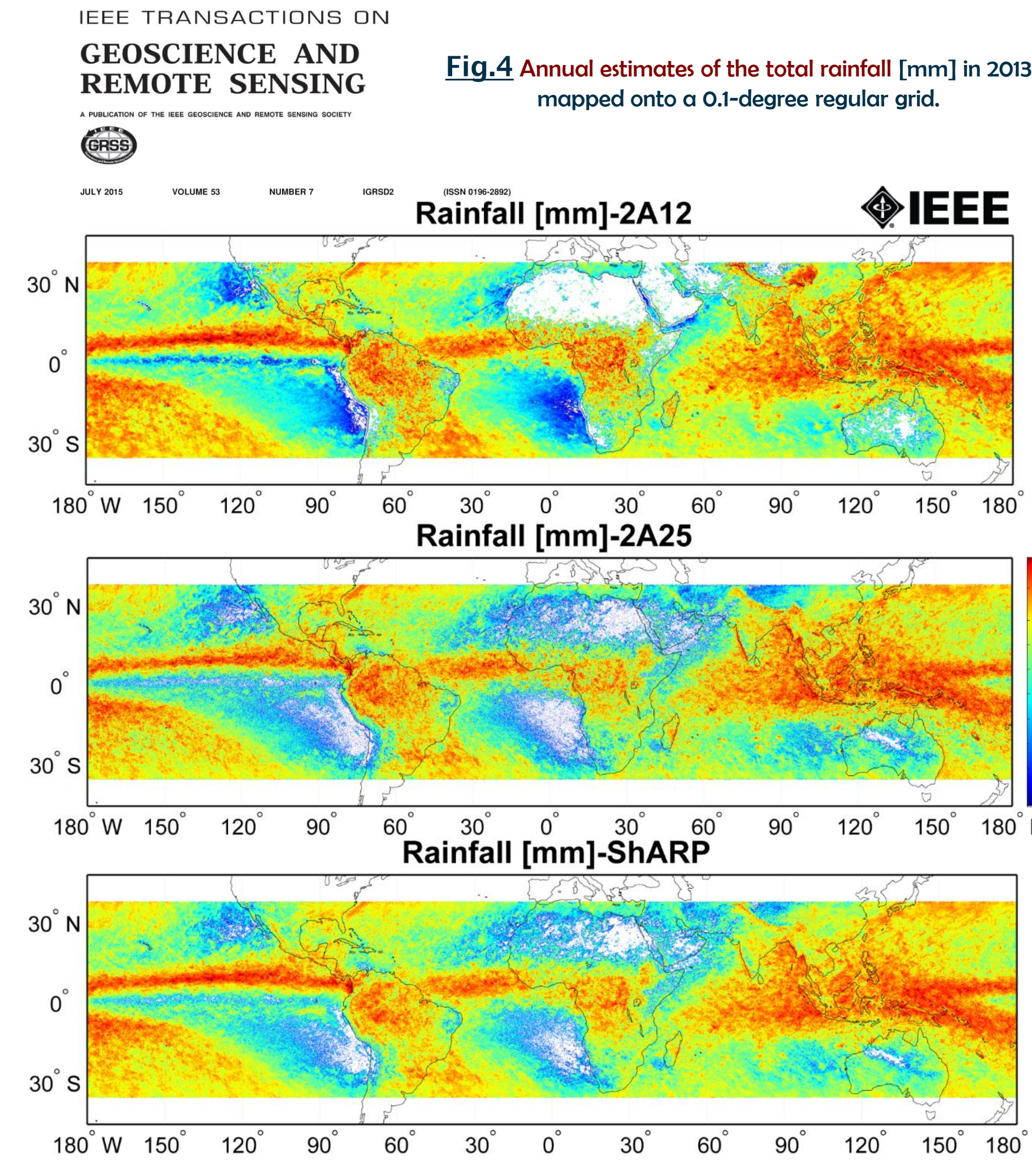


Fig.4 Annual estimates of the total rainfall [mm] in 2013 mapped onto a 0.1-degree regular grid.

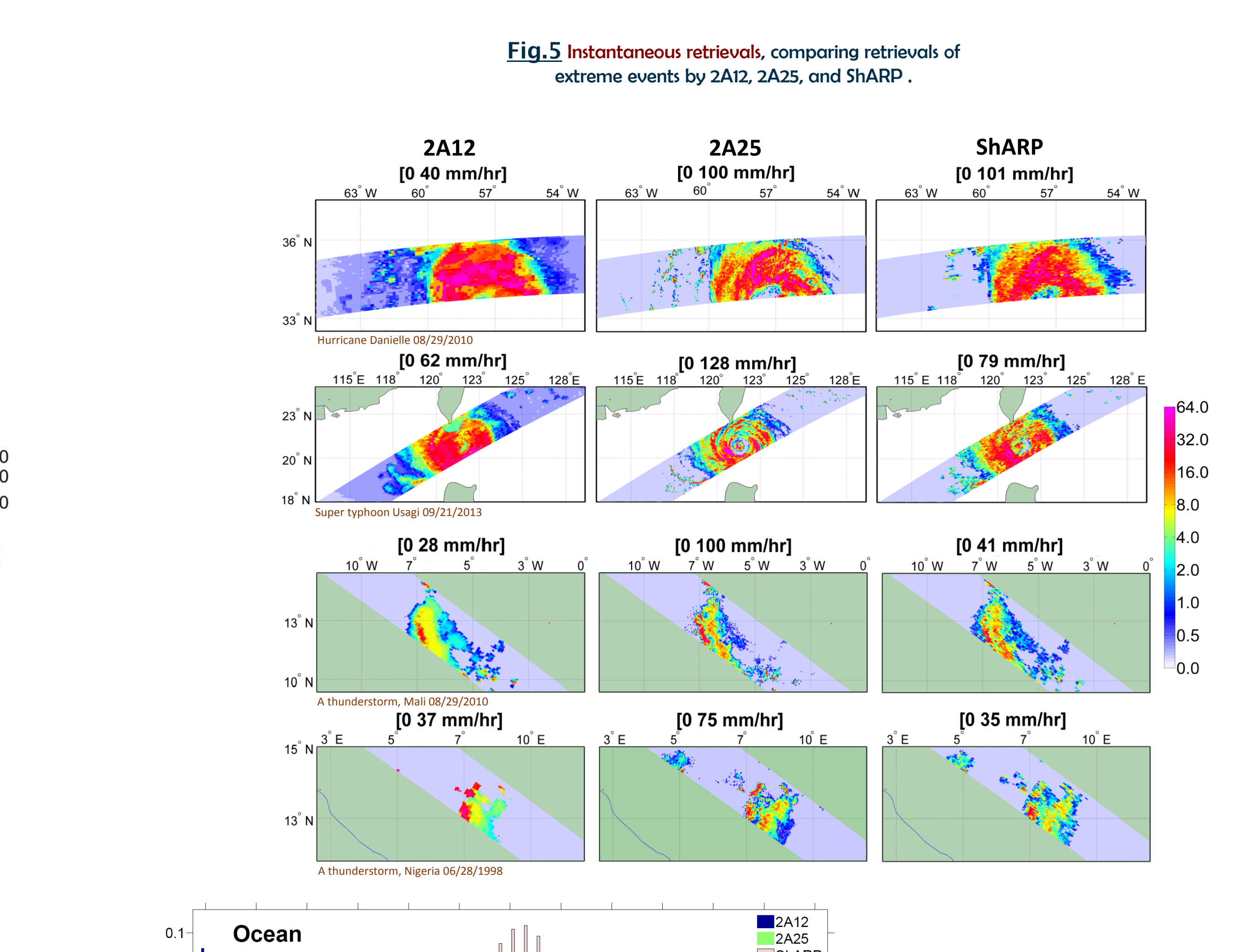


Fig.5 Instantaneous retrievals, comparing retrievals of extreme events by 2A12, 2A25, and ShARP.

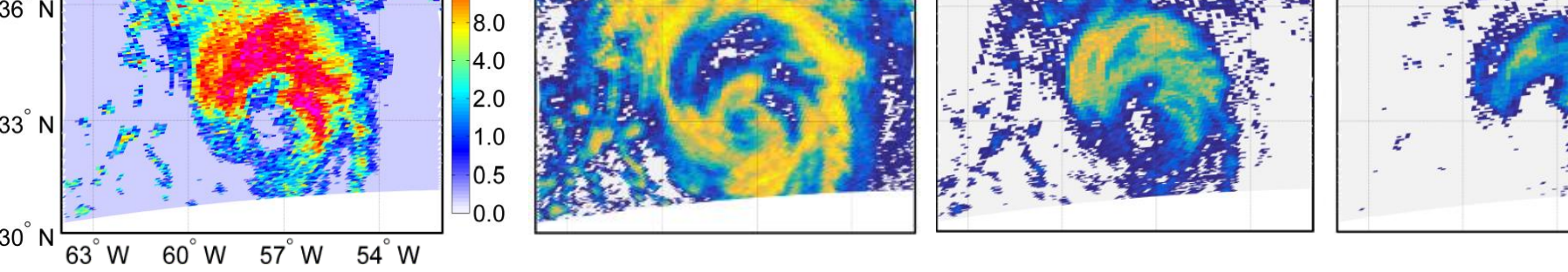


Fig.6 Probability maps showing different segments of the posterior probability density function for the ShARP retrieval of the hurricane Danielle (orbit No. 72840) at 09:48 UTC.

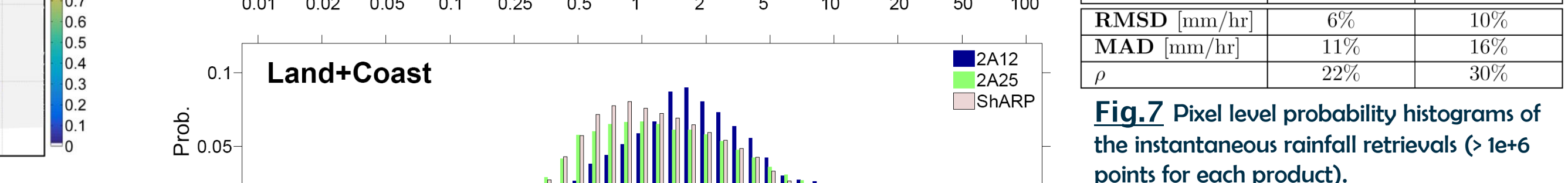


Fig.7 Pixel level probability histograms of the instantaneous rainfall retrievals (> 1e6 points for each product).

| Metrics      | Difference Metrics |      |
|--------------|--------------------|------|
|              | Ocean              | Land |
| RMSD [mm/hr] | 6%                 | 10%  |
| MAD [mm/hr]  | 11%                | 16%  |
| $\rho$       | 22%                | 30%  |

## ShARP: Complex Land Surfaces (coastal areas, snow-covered lands, and orographic precipitation)

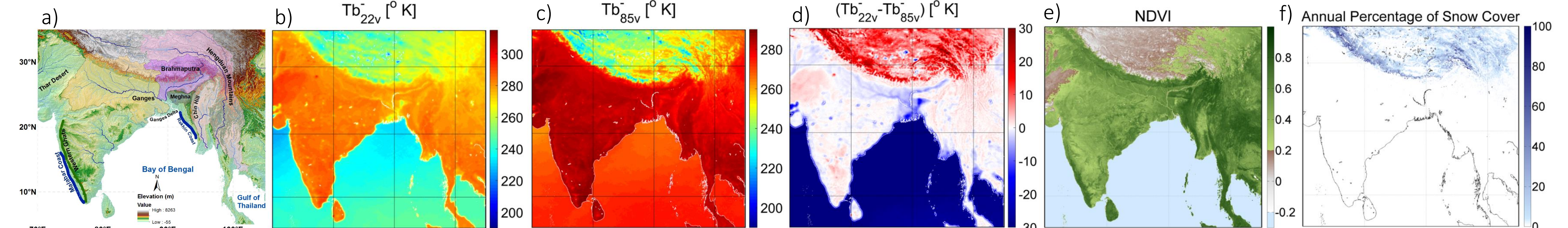


Fig.8 Study area (a), annual non-raining TMI-Tb values at channels 22v and 85v (b, c), the SI scattering index used in TRMM version 7 products (d), Normalized Difference Vegetation Index (e), and snow coverage (f) obtained from MODIS data in 2013

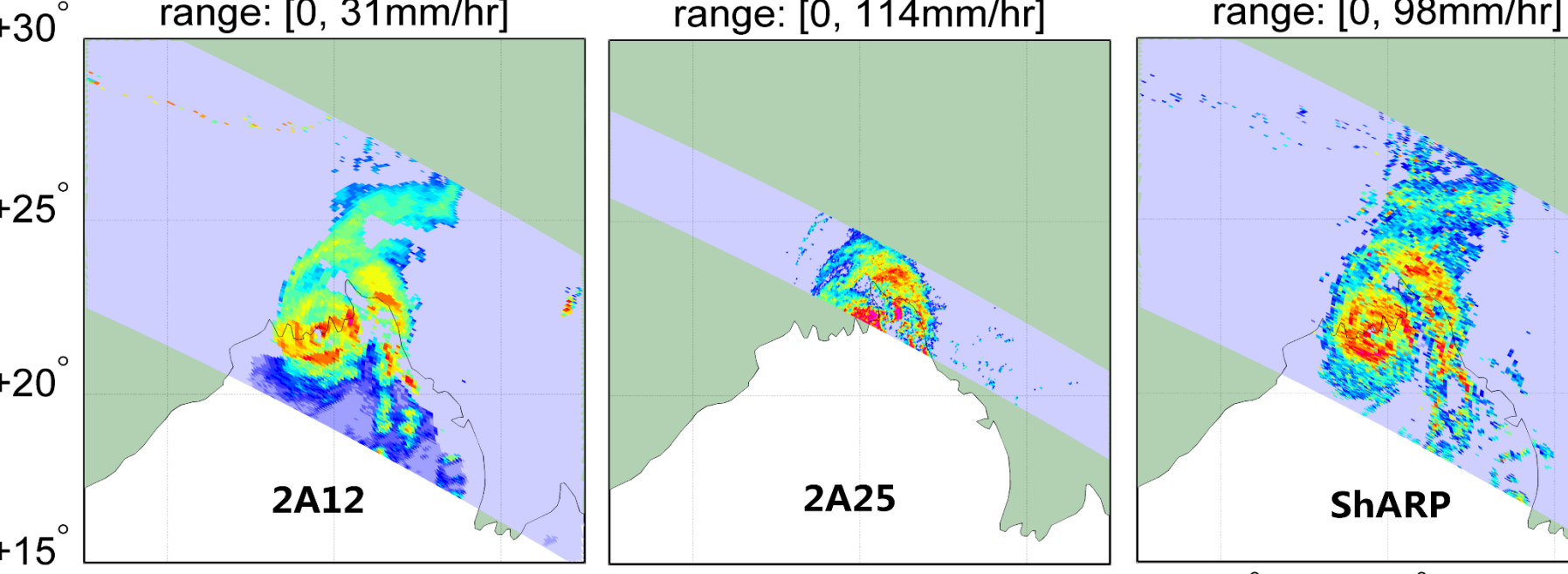


Fig.9 Rainfall retrievals for the TRMM overpass on November 15, 2007 capturing the cyclone Sidr at UTC 13:59, including the results from: 2A12 (left panel), 2A25 (middle panel), and ShARP (right panel). Histograms of the passive and active retrievals over land and coastal areas.

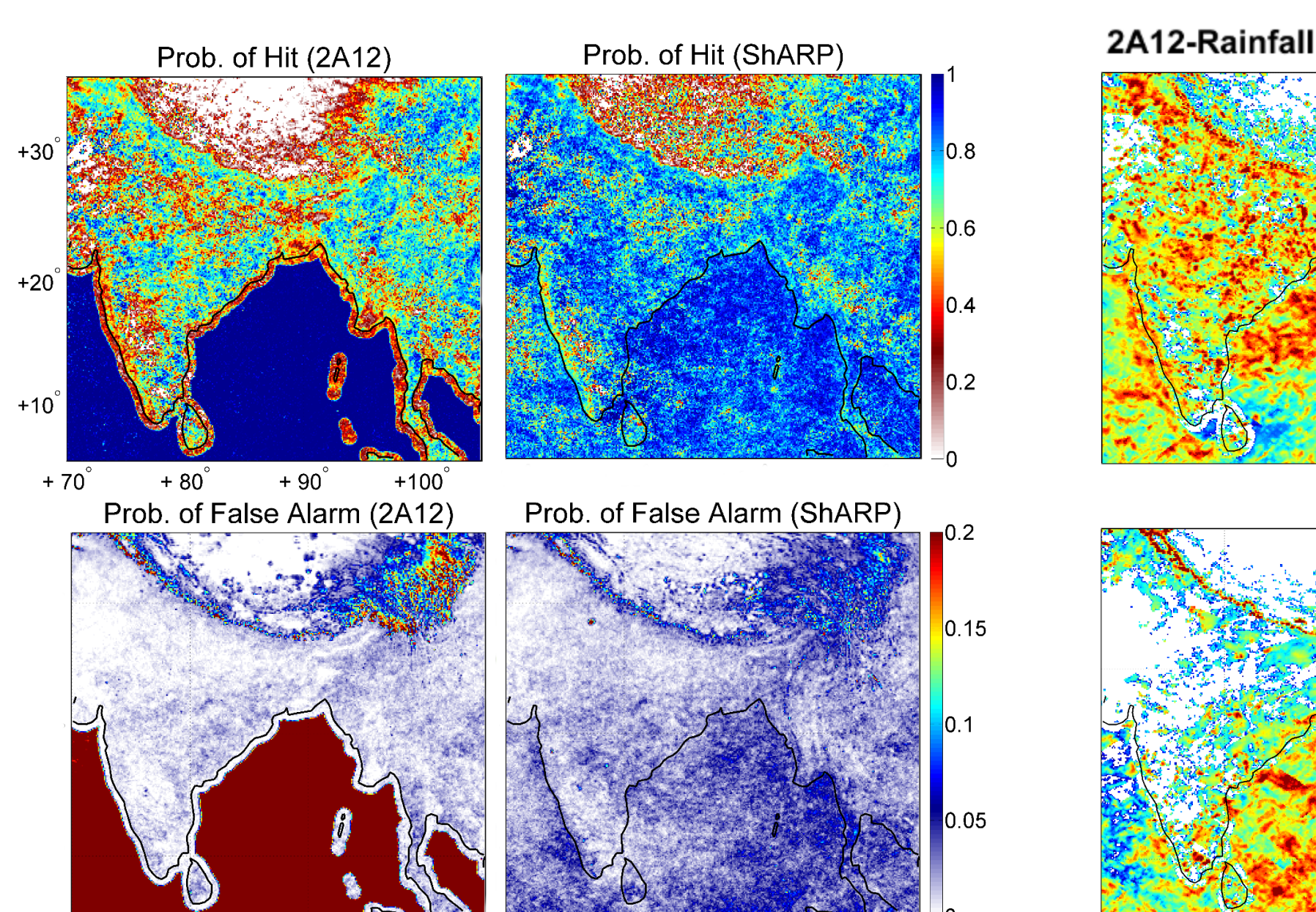


Fig.10 Improved retrievals over coastlines. Annual probability of hit and false alarm, comparing the 2A12 and ShARP retrievals with the 2A25 as a reference. The fields show probabilities obtained for all inner-swath overpasses in 2013 shown at 0.1-degree.

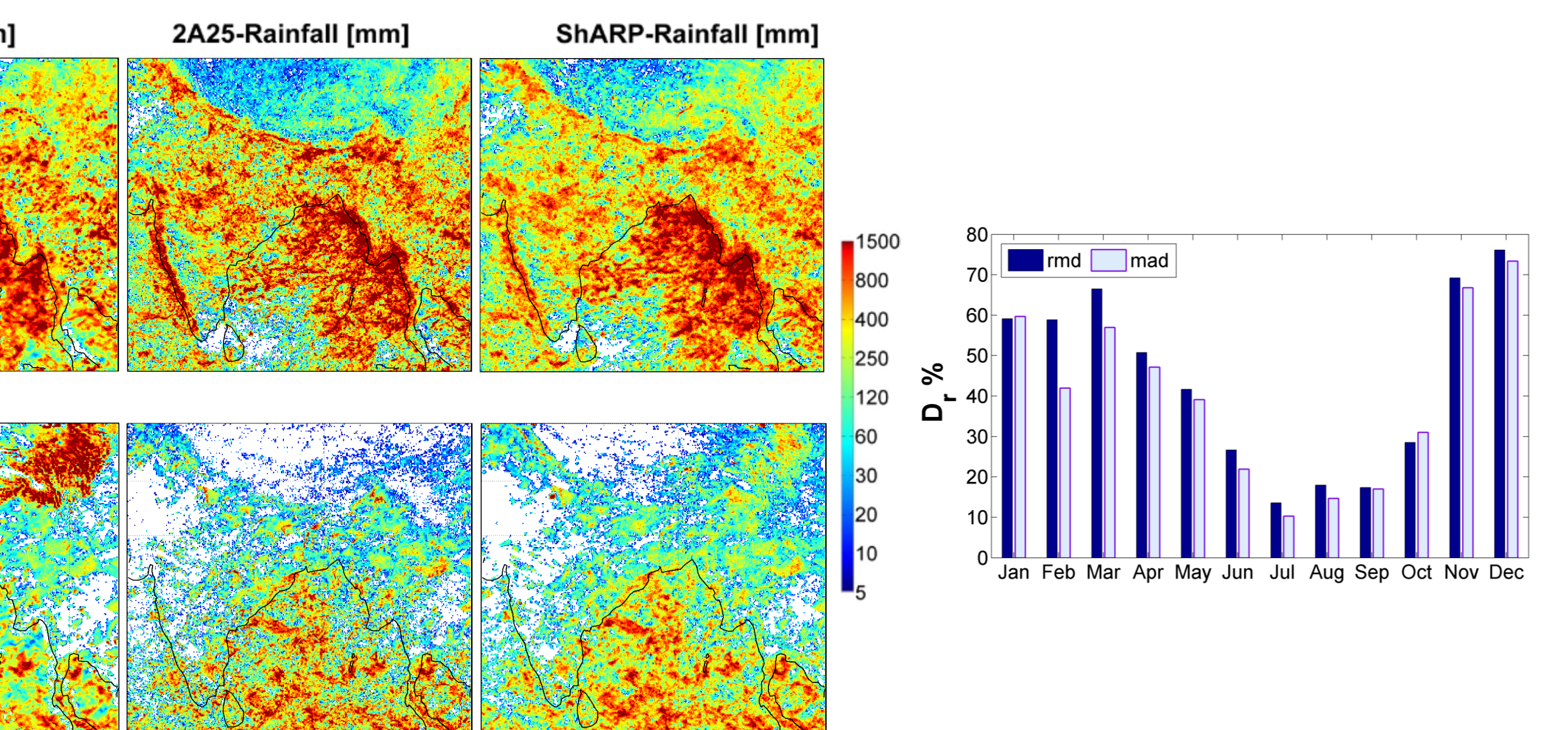


Fig.11 Improved retrievals over snow covered lands and orographic features. Monthly rainfall retrievals over the study region shown at 0.1-degree. First to the last rows contain three months accumulations of total rainfall (mm) for July-September (JAS) and October-December (OND) throughout the calendar year 2013. The results only contain the rainfall captured within the TRMM inner swath.

Fig.12 Improvement in error statistics. Top: relative reduction (Err%) in monthly root mean-squared difference (rmd) and mean absolute difference (mad) in ShARP land retrievals compared with the 2A12.

## New Directions

### Linking surface properties to hydrometeor profiles

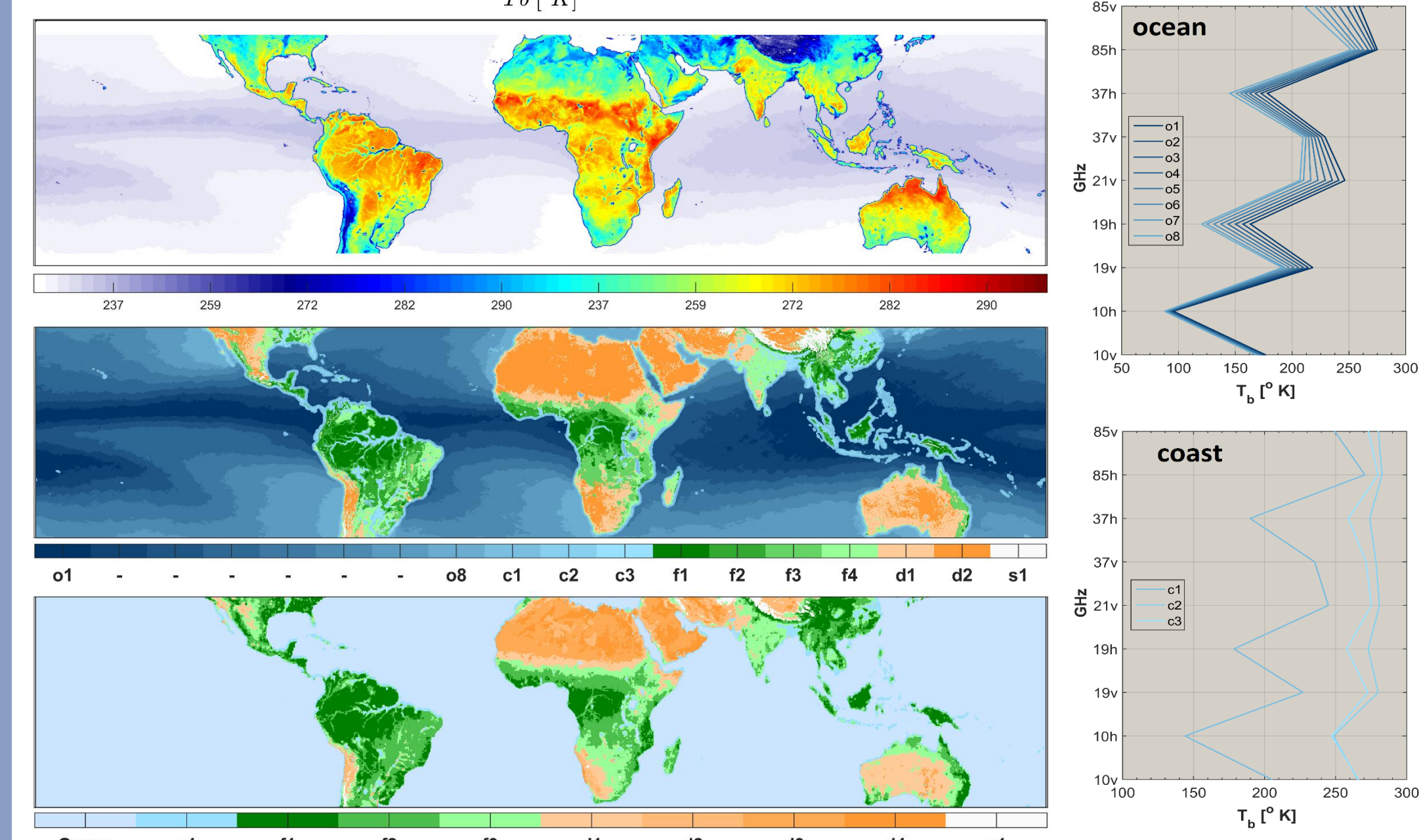


Fig.13 Land surface classes for database stratification. Top panel: Root mean squared  $T_b$  values of all TMI inner-swath overpasses in 2008. Middle panel: The k-means clustering of upwelling radiation. Bottom panel: Climatology of the AMSR-E surface emissivity classes used for comparison purposes. The "o", "c", "f", "d", and "s" symbols denote ocean, coastal, forest, desert, and snow-covered land-surface classes. Spatial mean values of the TMI radiometric brightness temperatures over different land surface classes. We can clearly see how different polarization features determine different land surface classes over land while over ocean transitional shifts in  $T_b$  values are the determining factor for proper classification.

### A formalism for retrieval + fusion

$$\text{minimize}_{\{c_i\}_{i=1}^{n_s}} \sum_{i=1}^{n_s} (y_i - B_S c_i)^T W_i (y_i - B_S c_i) + \sum_{i=1}^{n_s} \sum_{j=1}^{n_s} (y_i - B_S c_i)^T V_{ij}^{-1} (y_j - B_S c_j) + \lambda_1 \sum_{i=1}^{n_s} \|c_i\|_1 + \lambda_2 \sum_{i=1}^{n_s} \|c_i\|_2^2$$

$$\text{subject to } c_i \geq 0, \sum_{j=1}^{n_s} 1^T c_j = 1, \hat{x} = \sum_{i=1}^{n_s} R_S c_i \hat{e}_i$$

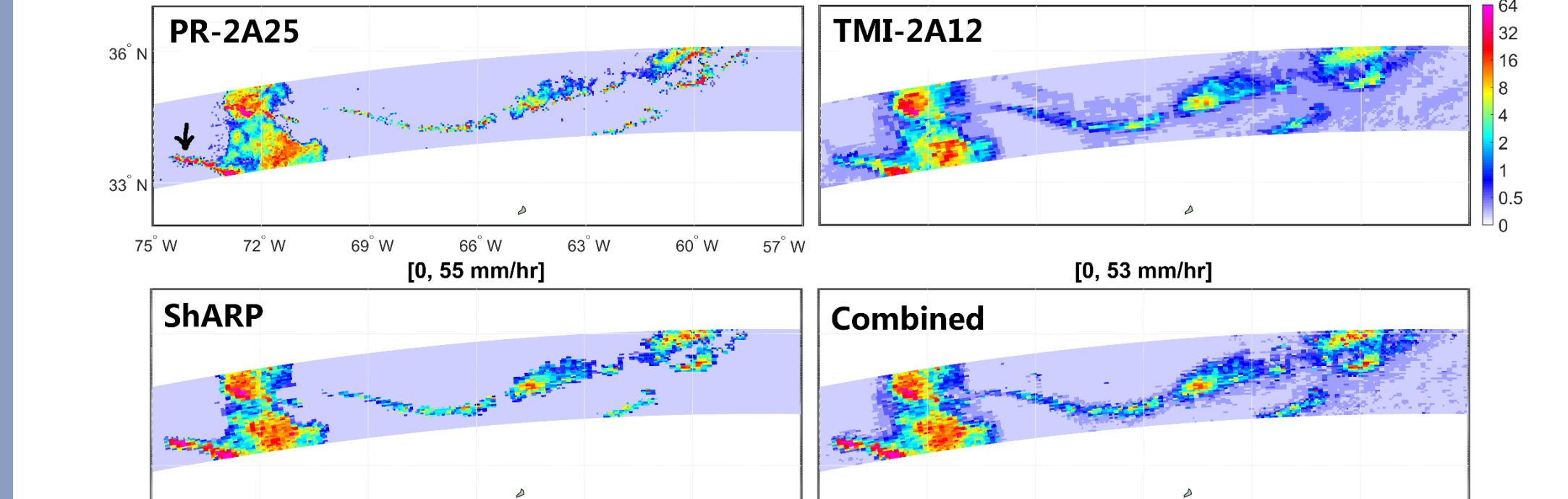


Fig.14 A proof of concept of the combined retrieval-fusion formalism that may allow us to improve retrieval of low and extreme precipitation. Shown are different retrievals of a storm captured in the TRMM orbit#03357 on 06/28/1998.

### Compact a priori databases and new algorithms

Note: Recent advances in estimation theory allows us to only estimate the representation coefficients for Bayesian precipitation retrievals but also approximate compact dictionaries and atoms of raining  $D_r^T$  and non-raining (dry)  $D_n^T$  upwelling microwave spectral radiation, using TRMM and/or GPM coincident radar/radiometer data. Here,  $\{b_i^d\}_{i=1}^M$  denotes a large number of raining (r) and non-raining (d) spectral Tb values for which we may estimate the Tb atoms in column space of  $D_r^T$  by solving the following non-convex optimization problem:

$$\text{minimize}_{\{c_i\}_{i=1}^M} \sum_{i=1}^M \|b_i^r - D_r^T c_i\|_2^2 + \Phi(c_i) \text{ subject to } c_i \geq 0, 1^T c_i = 1,$$

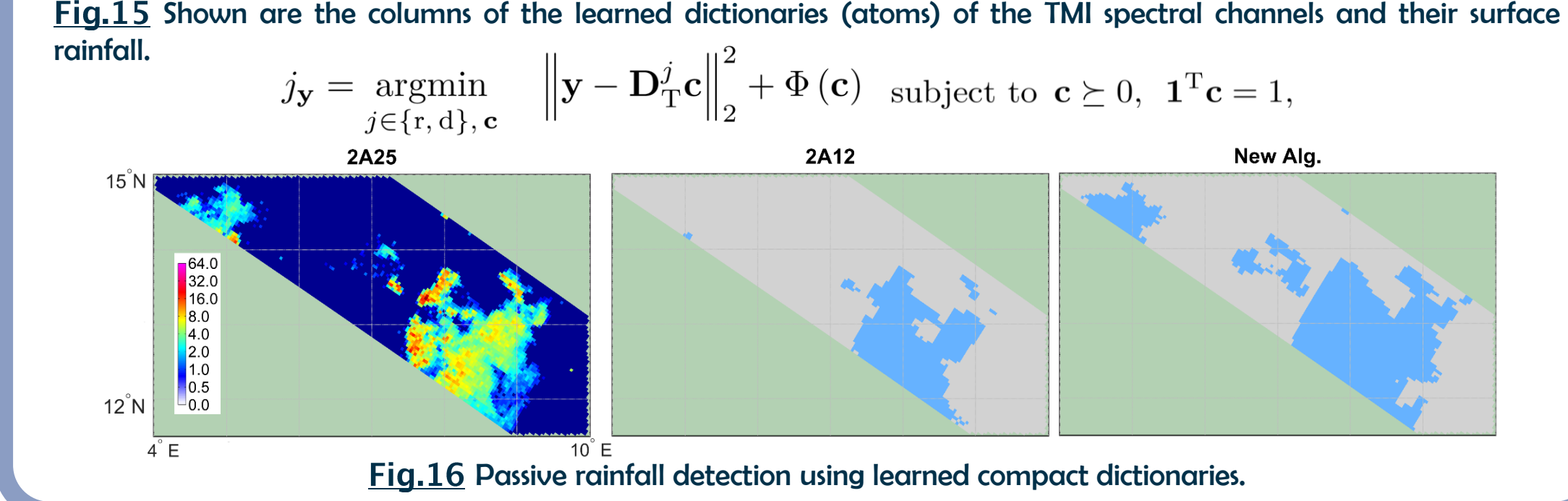


Fig.15 Shown are the columns of the learned dictionaries (atoms) of the TMI spectral channels and their surface rainfall.

$$j_y = \arg \min_{j \in \{r, d\}, c} \|y - D_r^T c\|_2^2 + \Phi(c) \text{ subject to } c \geq 0, 1^T c = 1,$$

Fig.16 Passive rainfall detection using learned compact dictionaries.

### Future Directions

- Proper linkage between the land surface geophysical parameters and hydrometeor profiles is needed to reduce regional biases over complex land surfaces.
- New regularization formalisms for combined retrievals in GPM era to not only retrieve but also integrate observations of different platforms in an optimal sense.
- Compact learning of rainfall atoms for efficient and accurate retrievals of light and extreme rainfall over complex land surfaces.

### Acknowledgment

This research is supported by two GPM grants NN13AG33C, NN13AH35G and the K Harrison Brown Family Chair funding.